JOURNAL OF GEOPHYSICAL RESEARCH, VOL. 92, NO. A4, PAGES 3155-3164, APRIL 1, 1987

ENERGETIC PARTICLE ABSORPTION AT IO

Andrew N. Wright[1]

The Blackett Laboratory, Imperial College, London

Abstract. The absorption of test particles is studied analytically for the Jovian satellite Io. Io, being a conductor, perturbs the ambient E and B fields in and near the magnetic flux tube that is connected to it. The work is a development of some very early work by Schulz and Eviatar (1977). This paper extends their analysis not only by including more completely the effects of the dipole geometry of the background fields and by treating all particle pitch angles, but also by not being restricted to the infinite satellite conductivity limit. We also take into account the effect of the perturbation varying in amplitude as it propagates through the Io torus. We show that the total energy sufaces of test particles can be used to understand how the different interaction regimes derived by Schulz and Eviatar arise. The theory also enables estimates of the energy range for each type of interaction to be made and can be applied to interpret particle distributions from Io's L shell. As an example, the electron distribution near Io's flux tube has been examined and features expected from the theory are found to be present.

Introduction

The motion of a satellite through a magnetosphere can be a signifcant loss mechanism for magnetospheric particles. If a particle's trajectory impinges on the moon, it is absorbed, and this mechanism is termed "satellite sweeping." The effect of a satellite is to provide a sink for particles which is commonly modeled in the radial diffusion equation in terms of a characteristic lifetime [Schardt and Goertz, 1983]. If the magnetosphere is in equilibrium, it is possible to make estimates of the radial diffusion coefficients if the loss rate of particles due to satellite sweeping is known [Mogro-Campero and Fillius, 1976; Thomsen et al., 1977; Hood, 1985; Bell and Armstrong, 1986; Paonessa and Cheng, 1986]. Previous models of sweeping have largely been concerned with gyrophase dependence when the Larmor radius is large, "leapfrogging" over the satellite, eccentricity of the orbit, and tilt of the orbit relative to the magnetic equator [Paonessa and Cheng, 1985, and references therein; Bell and Armstrong, 1986]. All of this work has assumed that the cross section which the satellite presents is simply its geometric cross section.

The interaction of the Jovian satellite Io with the Jovian magnetosphere is particularly complicated. This is partly because Io is not only a sink of particles, but also a source due to its volcanic activity. In fact it is the dominant source of plasma in the inner Jovian magnetophere [Belcher, 1983; Schardt and Goertz, 1983]. The flow of magnetospheric plasma near Io is complicated because of the currents that flow through Io [Goldreich and Lynden-Bell 1969; Neubauer, 1980; Wright and Southwood, 1987] and mass pickup process which also drives currents and transfers momentum between magnetospheric plasma and picked-up plasma [Goertz, 1980; Southwood and Dunlop, 1984]. These processes manifest themselves in electromagnetic fields that will influence energetic particle motion. The effect of Io's electromagnetic perturbation on energetic particles was first noted by Schulz and Eviatar [1977]. By means of a limited model, they showed that the effective cross section for absorption could be considerably modified from the geometric cross section. Their pioneering work made it clear that the cross section would depend upon the particle's charge, kinetic energy and electrical properties of the satellite. Subsequent studies by Goldstein and Ip [1983] have also discussed the motion of charged particles past Io.

In this paper we concentrate on the effect that Alfvén waves have on particle absorption. Several new features are added to the earlier work of Schulz and Eviatar that make the model sufficiently accurate to be useful in discussing particle motion past Io quantitatively. These new features are the inclusion of dipole geometry in the background field; the theory describes all pitch angles, and the satellite can assume any conductance. In addition, we qualitatively describe the effect of the variation of the wave fields along the Io flux tube. In order to simplify the problem we nelgect the offset and tilt of the Jovian magnetic field and assume that Io is confined to the magnetic equatorial plane. The small tilt of the Alfvén wings (8 degrees) is also neglected.

The model treats the particles as test particles whose orbits can be computed from adiabatic theory and should be appropriate to the high energy tail of the plasma distribution at Io provided the Larmor radii are small compared with the radius of Io. (Electron Kinetic energy is less than 10^3 MeV; proton kinetic energy is less than 0.2 MeV. For these energies the Larmor radius will be less than or equal to an Io radius.) Particles of these energies of these will not be sensitive to gyrophase effects. Higher energy particles will scatter in pitch angle, and particle depletion via the loss cone may become more important than satellite sweeping losses. Within this approximation the longitudinal distance drifted by electrons in one half bounce will be much less than an Io radius, and so an electron will be absorbed if its trajectory (mapped onto the equatorial plane) intersects Io. However, as Thomsen et al. [1977] point out, protons of low energy may enhance their lifetime by "leapfrogging" over satellite (e.g., 0.6 MeV protons have twice the expected liftime due to the leapfrogging effect). By considering the "bounce-averaged" perturbation experienced by particles that mirror at different latitudes we can qualitatively discuss the effect of nonuniform Alfvén wave propagation. We are able to maintain an analytical description throughout by introducing an empirical relation for the kinetic energy of the particle as a function of L shell under conservation of

[1]Now at Theoretical Astronomy Unit, School of Mathematical Sciences, Queen Mary College, London.

Paper number 6A8573.
0148-0227/87/006A-8573$05.00

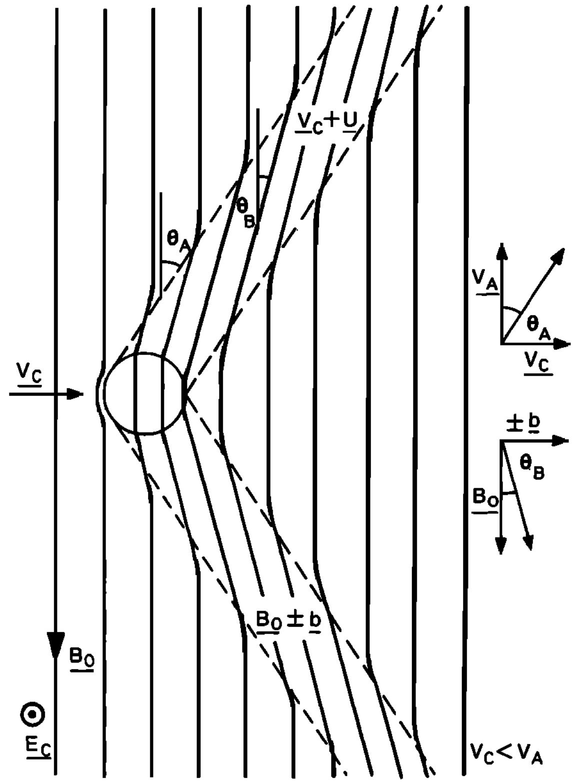

Fig. 1. The equilibrium of a conductor standing in a plasma flow: in the satellite rest frame, plasma is convected at V_c by the convection electric field E_c. The interaction produces perturbations to the electric, magnetic and velocity fields via the Alfvén waves. These waves propagate along the background magnetic field direction at the Alfvén speed (V_A) and are swept back past the satellite at the plasma convection speed. The two resulting stationary wave structures are inclined at an angle θ_A to the background magnetic field, where the Alfvénic Mach number is given by $M_A = \tan(\theta_A) = V_c/V_A$.

the first two adiabatic invariants [Hamilin et al., 1961; Southwood and Kivelson, 1975]. We also describe the motion of test particles past Io, and derive expressions for the cross section and rate of mass absorption as a function of kinetic energy and equatorial pitch angle. The results provide an explanation for some features seen in the Voyager 1 data during its pass of Io's flux tube.

Previous Studies

The simplest model illustrating the essential features of particle trajectories past Io is to treat the satellite as a perfect conductor and only consider particles having a pitch angle of 90°, as was done by Schulz and Eviatar [1977]. The interaction of a conductor with a corotating plasma is shown in Figure 1. The ambient plasma (and frozen in field) pass the satellite with a velocity, V_c, and in Io's frame there is an electric field, E_c,

$$E_c = -V_c \wedge B_0 \tag{1}$$

The positions of the field perturbations are marked by two structures extending away from Io and were termed Alfvén wings by Drell et al. [1965]. They are swept back in the flow at an angle θ_A to the background field given by

$$M_A = -V_c \;/\; V_A = \tan(\theta_A) \tag{2}$$

M_A is the Alfvénic Mach number and V_A the Alfvén speed. The wings thus align with the characteristics of the Alfvén wave [Neubauer, 1980; Wright and Southwood, 1987].

If Io (or its immediate atmosphere) is perfectly (infinitely) conducting, it could not sustain any internal electric field. The exterior electric field induced in Io's frame by the relative motion between Io and the corotating Jovian plasma would be strongly modified in order that it point normal to the outer boundary between the perfectly conducting region. However, as was first recongized by Goldreich and Lynden-Bell [1969], the field perturbation does not remain localized to Io. Alfvén waves can communicate the electric perturbation to large distances. The guided nature of the Alfvén wave imples that the disturbance remains localized in dimensions perpendicular to the field at any point. The theory is described in a variety of papers [Drell et al., 1965; Neubauer, 1980; Goertz, 1980; Southwood et al., 1980; Wright and Southwood, 1987].

Let us consider the nature of field and flow perturbations associated with the waves. The Alfvén Mach number at Io has been estimated by Southwood et al. [1980] and Acuña et al. [1981] to have a value of 0.15, which implies that the Alfvén wings are inclined at an angle of about 8° to the ambient magnetic field. We shall ignore this small tilt and treat the field perturbations as convected strictly parallel to the field. As the perturbation convects away from the near-equatorial regions, field and ambient plasma density variations will modify its amplitude. However, for near-equatorially mirroring particles (pitch angle near 90°) this is not important. This is the case treated by Schulz and Eviatar [1977], and before developing our more complicated model it is worthwhile to review their results.

Previous Alfvén wave models have shown that

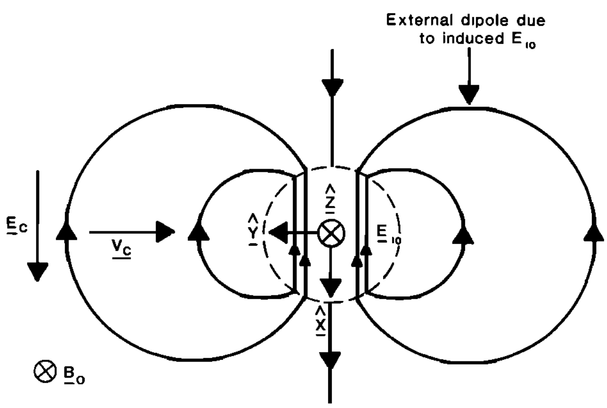

Fig. 2. The perturbing electric field due to Io's presence: The convection electric field experienced in Io's rest frame gives rise to a charge distribution on the surface of Io, or in Io's ionosphere. The associated electric field is shown and has a maximum magnitude (E_{I0}) that is a fraction of the convection electric field. Outside Io the charge distribution gives rise to a dipolar electric field perturbation. The orientation of the Io-centered coordinates (x,y,z) is also shown.

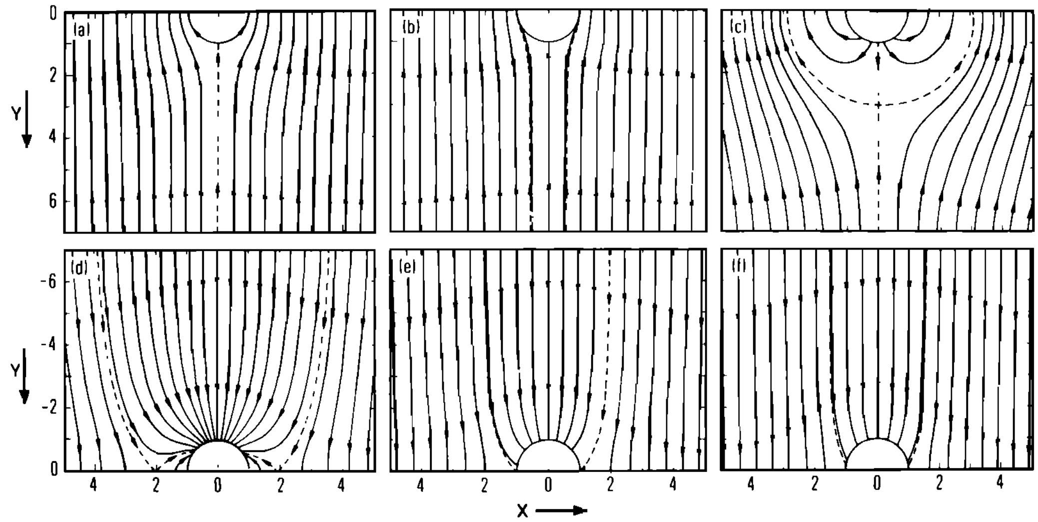

Fig. 3. Adiabatic drift paths past Io: The variety of different drift paths is shown for different species and kinetic energies [after Schulz and Eviatar, 1977]. In their model the trajectories can be classified as follows: (a) trajectory corresponding to zero kinetic energy ions or electrons; (b) type of trajectory for all ions with nonnegligible kinetic energy (the degree to which the trajectories deviate from those in Figure 3a increases with kinetic energy); (c– f) trajectories describing electron motion with increasing kinetic energy. It can be seen that the direction of background electron drift changes between Figures 3c and 3d. This is because the increase in kinetic energy causes the magnetic field to dominate the electric field drift. The orbit and energy classifications in this figure carry over to the more complex model described in this paper. Details of the classification as a function of kinetic energy, equatorial pitch angle, and charge are delineated in Table 1.

perturbations external to Io and the Alfvén wing are two dimensional and dipolar. This is shown in Figure 2. The dipolar perturbation electric field, unlike the corotational electric field, has a nonzero azimuthal (y) component and causes particles to drift radially (in x). It is this that strongly modifies the cross section for particle absorption from being the geometrical cross section. Evidently a zero– energy charged particle moving only under $E_\wedge B$ drift avoids the obstacle entirely if the external field is precisely canceled at the obstacle. In general the degree to which particles deviate from their unperturbed trajectories is a function of their pitch angle, charge and energy. Figure 3 shows the different guiding center trajectories calculated by Schulz and Eviatar [1977] for various electron and proton energies. The assumed fields are given by

$$\begin{aligned} \Phi &= -xE_cR_I\,.\,[1-1/(x^2+y^2)] \qquad r>R_I \\ B_z &= B_{eq}(1-3x.R_I/R_JL_I) \qquad r>R_I \end{aligned} \tag{3}$$

where Φ is the electric potential; R_J is one Jovian radius; L_I is the mean L shell of Io's orbit; B_{eq} is the ambient field at Io; R_I is the cross section of the obstacle projected into the plane perpendicular to B_{eq}; x and y are normalized to R_I and x is directed radially. The field is assumed to be in the z direction. The second term in the magnetic field expression is designed to take account of the radial gradient in the background field. The form of the potential is such as to reduce the tangential field to zero on a circle of radius R_I. The drift paths shown in Figure 3 are qualitatively like those that will occur for all pitch angles, but we need to develop the model further if we are to describe particles of general pitch angle. The more detailed model that we present in the next section produces flow paths of the same topology as those in Figure 3. We show how the type of flow executed by a particle is dependent upon its charge, kinetic energy, equatorial pitch angle and the nature of Alfvén wave propagation through the Io torus.

General Conductor Model With a Three– dimensional Perturbation

The Schulz and Eviatar treatment is limited in several ways. The effective conductance of Io is not infinite. We thus give a treatment in which the satellite is allowed to assume any degree of conductivity. Next, as we have mentioned, Schulz and Eviatar's treatment is only valid for near– equatorially mirroring particles (90° pitch angle). We show how particles of all pitch angles can be treated. We derive orbits by conserving μ and J, the first and second adiabatic invariants, rather than just the magnetic moment.

As particles with small pitch angles mirror far from Io, in their bounce motion they sample the perturbation fields far from Io. As we have noted, the magnitude of the perturbations is not uniform along the Alfvén wings. We shall allow for the effect of wave field amplitude variation along the background field direction.

When treating particles that have nonzero mirror latitudes the system is no longer two dimensional. However, it is still convenient to use the frame described in Figure 2 if we think of the $\hat{z}$ direction as always lying along the ambient magnetic field direction. Now z represents the distance along the field line rather than height above the magnetic equatorial plane. We shall continue to work in this plane and identify the particle drift trajectories by their L shell, or x values, when at the magnetic equator.

Let us now consider the perturbation produced by a general conductor, and then discuss how this propagates along the field line. If Io does not have infinite conductivity, the plasma flow and ambient field will not be completely excluded from it. By closing the field-aligned Alfvén currents through the body of Io, or its ionosphere, we find that the perturbation to the flow at Io is given by [c.f. Southwood and Dunlop, 1984]

$$u = -[\Sigma_I/(2\Sigma_A+\Sigma_I)].V_c \qquad (4)$$

The Alfvén conductance of the plasma (Σ_A) and ohmic conductance at Io (Σ_I) determine the magnitude of the disturbance to the corotation flow. One may confirm that the perfect conductivity limit is recovered by setting Σ_I infinte and conversely in the perfect insulator limit ($\Sigma_I = 0$) as expected.

Predicting the manner in which the wave amplitude varies along the field is difficult; it is a function of the scale over which the flow near Io is disrupted and could range from an Io diameter to very much larger if mass pickup dominates the effective conductivity [see Southwood and Dunlop, 1984]. If the scale length of the Alfvén wave is much smaller than that of the density profile, we should expect the WKB limit to apply. In this limit the amplitude of the velocity perturbation is inversely proportional to the fourth root of the mass density [Alfvén and Falthammar, 1963]. In this case, the dominant change in amplitude takes place on exiting the torus where the perturbation may increase by a factor of about 4 (F. Bagenal, private communication, 1985). In the opposite extreme, when the scale length of the wave is much greater than the density distribution, significant reflection may be anticipated at the torus edge and the transmission coefficient (of the velocity perturbation) would be proportional to the ratio of interior to exterior magnetic field strength. In any event there will be a variation of Alfvén wave amplitude with magnetic latitude (i.e., z) with the largest change probably occurring at the edge of the torus. Due to the enormous increase in magnetic field strength with latitude the Alfvénic electric field is almost certain to increase with latitude also.

We model the effect of an amplitude variation along B by introducing the idea of a "bounce-averaged" perturbation. In this approach the geometry in Figure 2 is maintained, yet the model is three dimensional (the extra dimension implicit in the bounce-averaged term).

The form of the electrostatic potential is

$$\Phi = \Phi_I - E_c R_I x \qquad (5)$$

where Φ_I is the perturbation potential that a particle experiences. Approximating this to a two-dimensional dipole it can be written as

$$\Phi_I = h(\alpha_0, u).E_c R_I x/(x^2+y^2) \qquad (6)$$

The model of Schulz and Eviatar can be recovered by setting the scaling factor, h, to unity (α_0 is the equatorial pitch angle of the particle). The factor h can be written in the following way:

$$h(\alpha_0, u) = [u/V_c].\langle E_0(\lambda)\cos^3\lambda\rangle/E_{I0} \qquad (7)$$

(λ is the magnetic latitude; E_{I0} is the perturbation electric field amplitude inside Io, and $E_0(\lambda)$ is the amplitude at a latitude λ). The square bracketed term in (7) represents the effect of the finte conductance. The second term is the bounce-averaged perturbation — the $\cos^3\lambda$ weighting factor is to allow for the rate of L shell crossing varying with latitude in a dipole magnetic field for a given electric field. (It takes into account the convergence of magnetic field lines and the change in magnetic field strength.)

The bounce-averaged perturbation is of central importance to our model. The value h will have for a given particle depends upon the following factors (see equation (7)): the size of the perturbation produced by Io (i.e., u/V_c) or the satellite conductance); the variation with latitude of the Alfvén wave structure — especially the size of the electric field; and the latitudes that the particle can access (determined by its equatorial pitch angle). For example, if Io is an insulator (u=0), then $E_0(\lambda)$ would be zero for all λ, and all particles would experience no perturbation (h=0). On the other hand, if Io is a good conductor ($u \approx V_c$) and the Alfvén waves obey the WKB limit (i.e., $E_0(\lambda)$ increases with λ), then h will not be zero. Particles confined to the equatorial plane would have h=1 (neglecting reflection from the Jovian ionosphere). Particles mirroring outside the equatorial plane will see larger electric fields, and h may exceed unity. The factor h may be computed in principle for a particle of any pitch angle by integration along its bounce orbit. Such an integration takes care of the amplitude variation along the field in the wave. Thus for any model of wave evolution one may compute h and thus reduce the problem to two dimensions; once h is known, one may project the particle drift trajectories onto the equatorial plane. The approach breaks down if the azimuthal drift in one half of the latitudinal bounce period exceeds an Io radius, a condition roughly equivalent to requiring the particle Larmor radius to exceed an Io radius. The critical energies for electrons and protons are 10^3 MeV and 0.2 MeV respectively. Above these energies absorption is gyrophase dependent and no longer treatable using adiabatic orbit theory.

Orbits in the (x,y) plane are given by

$$w(x) + q\Phi = \text{constant} \qquad (8)$$

where Φ is the total electrostatic potential including the effective wave potential described above. Φ is thus pitch angle dependent in addition to depending on x and y. The particle kinetic energy is w. Its dependence on the x coordinate is given by the requirements that the particle conserve the adiabatic invariants μ and J. The x dependence is evidently a function of equatorial pitch angle and is complicated in general. By assuming the Jovian magnetic field to be dipolar we can use the energy-L relation derived by Southwood and Kivelson [1975] on the basis of earlier computations of particle drift speed pitch angle dependence given by Hamlin et al. [1961].

$$(\partial w/\partial L)_{\mu,J} = -(2.1+0.9\sin\alpha_0).w/L \qquad (9)$$

The bounce-averaged drift velocity in the equatorial plane can be written as

$$V_D = B_{eq}\wedge\nabla(\Phi+w(x)/q)/B_{eq}^2 \qquad (10)$$

Trajectories can be produced by starting a particle far

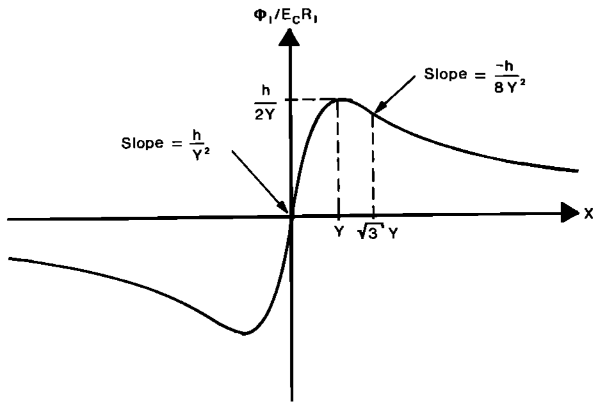

Fig. 4. The variation of the perturbing potential (Φ_I) in the equatorial plane is shown with x at a given y value (i.e., a given distance upstream or downstream from Io). The location of extrema and points of inflection are dependent upon y, as are the magnitude and gradient of Φ_I.

away from Io with an initial x value x_i at $(x_i, \pm\infty)$. This defines the total energy (w_{TO}) of the particle to be

$$w_{TO} = w(x_i) - qE_C R_I x_i \tag{11}$$

As the particle approaches Io, Φ_I needs to be included in the potential (equation (6)). The trajectory is defined by requiring constant total energy

$$w_{TO} = w(x) - qE_C R_I x + qE_C R_I hx/(x^2+y^2) \tag{12}$$

Expanding w(x) to first order about x_i and using the expression for $\partial w/\partial L$ (since $x = R_J(L-L_I)/R_I$) we can combine (10) and (11) to give

$$(x-x_i).[qE_C R_I + (2.1+0.9\sin\alpha_0)w(x_i)R_I/R_J L_I] - qE_C R_I xh/r^2 = 0 \tag{13}$$

It is convenient to normalize the energy terms in (13) by dividing through by $qE_C R_I$. We define the normalized quantity W to be

$$W = (2.1+0.9\sin\alpha_0).w(x_i)/(qE_C R_J L_I) \tag{14}$$

This yields the following expression describing the drift paths of particles:

$$W_{TO} = xh/r^2 - x[W+1] = -x_i[W+1] \tag{15}$$

where W_{TO} is the normalized total energy. Note that W is positive for protons and ions, and negative for electrons.

Contours of W_{TO} in the (x,y) plane give the trajectories of particles in the guiding–center approximation. If plotted, these would be similar to those shown in Figure 3. However, we can gain more insight into the problem from the construction of graphical solutions. To do this we take a value of y and plot the variation of total energy (W_T) (the central expression of (15) with x. This allows us to see where a particle of a given total energy (W_{TO}) is located at a given y. Before doing this let us consider the potential term alone. In Figure 4 the potential is shown as a function of x at constant y. It can be seen that the location of the extremum and points of inflection are dependent upon y. Also, the amplitude and gradients of the curve are determined by y, as indicated. It will be shown that the (maximum) values of the slopes at x = 0 and x = $\surd 3.y$ are important in determining the flow pattern. Clearly as $y \to 0$ we get singular values (at x=0) that tend to infinity. However, the expression for the potential is valid for $r^2 = x^2+y^2 \geq 1$, and since particles cannot access the region inside this, we have a well–behaved potential. It can easily be shown that the maximum slope at x = 0 is at (0,1) and has a value of h. The maximum slope of the point of inflection occurs at $(\surd 3/2, \frac{1}{2})$ and has a value of $-h/2$.

The relative magnitudes of the two terms in the center of (15) (i.e., how much influence the perturbation will have upon the particle) will determine how much the particles deviate from corotational trajectories and which type of flow (Figure 3) characterizes their motion.

For example, let us consider a very energetic particle that is positively charged. In this case the term $-x[W+1]$ will dominate. This situation is depicted in Figure 5a. The coarse–dashed line corresponds to $-x[W+1]$, and the solid line to the total energy curve at some value of y. When the particle is at y = $\pm\infty$, the perturbation contribution is negligible, and so the total energy curve will initially lie on the coarse–dashed line. The fine–dashed lines are lines of constant total energy. Starting a particle at a specific x value assigns a total energy value to it. As the particle moves nearer to Io, the total energy curve deviates from the dashed line, as indicated. The arrows show the motion of the particle across L shells that is required for it to maintain the same total energy. Therefore this diagram represents particle repulsion like that shown in Figures 3a and 3b. The condition to get this mode is that the total energy curve does not cross the x axis (except at x = 0). This is always satisfied if the slope of the coarse–dashed line always exceeds $\partial\Phi_I/\partial x$ at x = 0. So, particle repulsion always occurs if

$$1 \leq [W+1]/h \tag{16}$$

If we define x_∞ to be the maximum value of x (at y = $\pm\infty$) where a particle can be started and then suffer absorption at Io, we clearly need to trace back the limiting trajectory that passes through (1,0), for this mode. Using (15) we find that

$$x_\infty = 1 - h/[W+1] \tag{17}$$

and it lies between 0 and 1.

On decreasing [W+1] below the range given in (16), Φ_I will have more influence, and total energy surfaces like that shown in Figure 5b will result. It can be seen that particles approaching from y = $+\infty$ are excluded from a circle of radius $r_0{}^2 = h/[W+1]$ centered on Io. The trajectories that do exist inside r_0 are bound to Io. This mode is shown in Figure 3c, and as predicted from the form of the total energy surface, particles are repelled and have a cross section equal to zero. This type of flow will occur if [W+1] is positive, but not so large that the gradient of the perturbation potential at x = 0 will never dominate. This corresponds to the range

$$0 < [W+1]/h < 1 \tag{18}$$

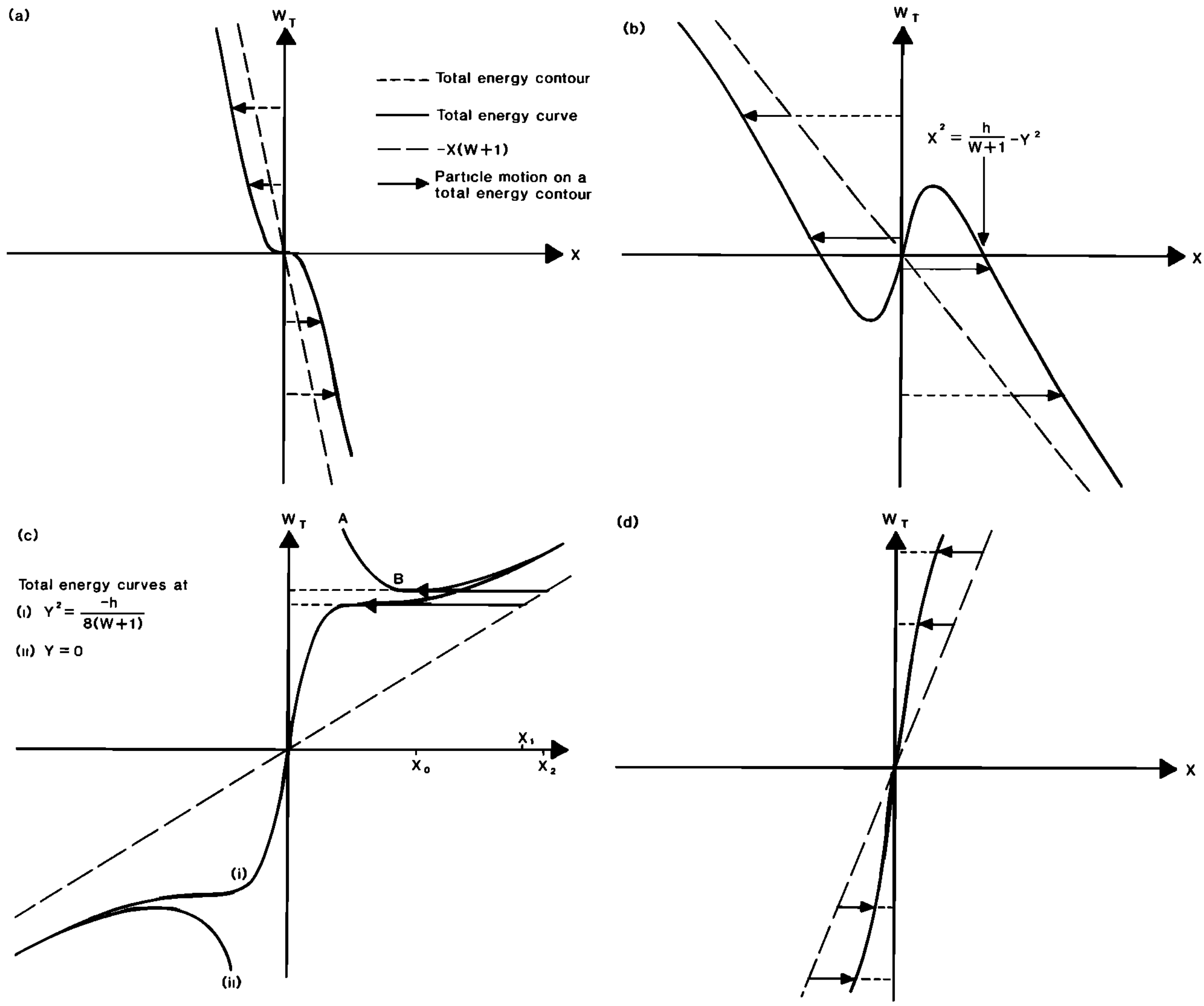

Fig. 5. Cuts through energy surfaces in x at constant y. In each figure the coarse–dashed line is the total energy curve at $y = \pm\infty$, and the thick solid lines are total energy curves at smaller values of y. Total energy contours are designated by the fine–dashed line. The x motion of particles (at constant total energy) that approach from $y = \pm\infty$ is represented by solid arrows. By studying the x displacement in these figures it is possible to identify the flow path topologies depicted in Figure 3, namely that Figure 5a describes Figures 3a and 3b; Figure 5b corresponds to Figure 3c and the exclusion radius is given by $r_0^2 = x^2 + y^2 = h/[W+1]$; Figure 5c describes Figure 3d; and Figure 5d corresponds to Figures 3e and 3f. Features of the two diagrams are discussed in the text and summarized in Table 1.

The remaining energy intervals are for [W+1] negative. It is easiest to treat the large negative values of W first. This will describe energetic electrons. The total energy surfaces that are produced will be similar to the one shown in Figure 5d. This corresponds to particle attraction and an enhanced cross section. The flow patterns are illustrated in Figure 3e and 3f. To produce this type of total energy surface the coarse–dashed line of Figure 5 must always dominate the slope at the point of inflection. This defines the energy range

$$[W+1]/h < -\tfrac{1}{2} \qquad (19)$$

By tracing the grazing trajectory back to $y = -\infty$, we find that

$$x_\infty = 1 - h/[W+1] \qquad (20)$$

which means that x_∞ lies in the range $1 < x_\infty < 3$. Note that the motion of electrons in this range is in the opposite direction to corotation. This is because the drift due to gradients and curvatures in the Jovian magnetic field is in the opposite sense to the plasma flow, and since these drifts are proportional to the particle's kinetic energy, they dominate when W is large and negative.

A reduction in particle energy from the case of extreme negative W leads us to the last energy regime. This interval is characterized by the slope at the point of inflection becoming dominant at some value of y. The total energy surfaces that describe the particle motion are like those shown in Figure 5c. This is the most subtle flow pattern to understand from the form of the total energy surface. The first curve in Figure 5c is plotted at $y^2 = [W+1]h/8$, i.e., where the slopes of $-x[W+1]$ and the point of

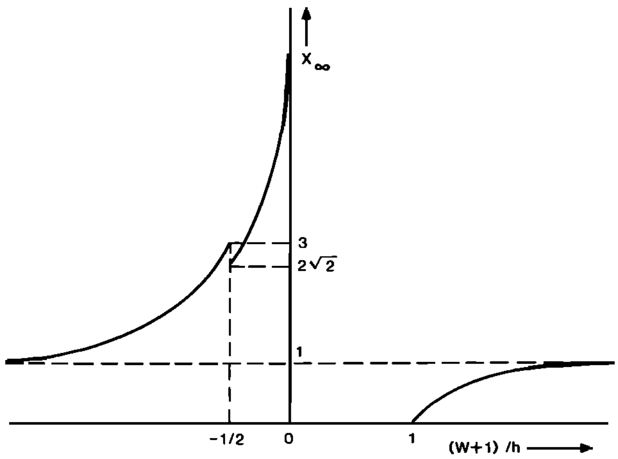

Fig. 6. The variation of x_∞ with [W+1]/h: The cross section for absorption of particles is given by $2x_\infty$. At high kinetic energies this tends to the geometric cross section, but at lower energies there is considerable deviation. For some particles the cross section is greatly enhanced, while for others it is zero.

inflection in Φ_I just cancel. Curve ii is the most extreme total energy surface, which occurs at $y = 0$. It is easy enough to see what happens to particles that start at $y = -\infty$ with $x < x_1$, and also for those with $x > x_2$. For particles that have an initial coordinate between x_1 and x_2 it is necessary to know in detail how curve i transforms to curve ii. The change from one to the other is smooth, the essential features being characterized by the extrema and inflections. The point of zero gradient on curve i bifurcates into a maximum and a minimum with a point of inflection between them. On approacing Io the minimum moves outward to larger x, and the maximum to smaller x. If we consider a particle that started between x_1 and x_2 (at $y = -\infty$), its motion is straightforward on moving to smaller y until the minimum in the total energy curve reaches the particle's total energy. Once this happens there is no (meaningful) solution if Io is approached futher. This is becaue the particle is turned around by the minimum and now moves to larger y. So the total energy curve now begins to collapse back to curve i as the particle recedes from Io. During this stage the particle will continue to move to smaller x until the descending peak of the total energy curve is equal to the particle's total energy. If motion away from Io is continued, no solution exists, and hence the motion has been reversed again (by the maximum this time). The particle continues to move toward Io, and the total energy curve continues to transform to curve ii. Thus particles that start at $y = -\infty$ with $x < x_1$ are simply attracted on approaching Io. Particles that begin with $x_1 < x < x_2$ will always move to smaller x, but the direction of their y velocity changes on encountering the maximum and minimum of the total enrergy surface. Particles can only exist on the portion of the total energy curve between the maximum and minimum after having been reflected onto it. Therefore the portion of the curve AB (Figure 5c) cannot be populated by particles form $y = -\infty$. Ths part of space will contain closed trajectories that are bound to Io. The gradient of the total energy curve at (1,0) is always negative (in the range $-h \to -h/2$). Hence the maximum lies inside Io, and any particle starting with $x < x_2$ will be absorbed. For particles with an intial x greater than x_2 there will be no absorption. This is because the minimum in the total energy curve ii is at

$$x_0 = (-h/[W+1])^{\frac{1}{2}} \tag{21}$$

For this type of flow ([W+1] negative, but $\partial\Phi_I/\partial x$ at the point of inflection dominates) we satisfy

$$-\tfrac{1}{2} < [W+1]/h < 0 \tag{22}$$

This limits the values that x_0 can take, and (22) implies that $\sqrt{2} < x_0 < \infty$. Thus x_0 is always greater than unity, i.e., it lies outside Io. The flow pattern for this energy regime is shown in Figure 3d. On examining this pattern it is possible to see the form of the locus of the minimum, which ends up at the flow singualrity at $(x_0,0)$. (The locus of the maximum is largely within Io for this particular example.)

By mapping back to $y = -\infty$ the limiting trajectory from $(x_0,0)$ we find an expression for the cross section.

$$x_\infty = 2.x_0 = 2.(-h/[W+1])^{\frac{1}{2}} \tag{23}$$

Figure 6 graphically shows the (schematic) variation of x_∞ with energy (W is positive for protons and ions, and negative for electrons). The kinetic energy corresponding to $|W| = 1$ lies in the range 16–23 MeV, the actual value being determined by the equatorial pitch angle (see equation 14)). Figure 6 can be used to construct the cross sectional variation shown by Thomsen [1979] who considered two different satellite conductivities.

Although the cross section for electrons with $W = -1$ is infinite, the rate of absorption is actually zero (in equilibrium). This is because the drift due to corotation is exactly canceled by gradient and curvature drifts, and hence there is no background drift with respect to Io. In this case the change in kinetic energy (demanded from conservation of μ and J) is exactly met by the change in electrostatic potential energy supplied by $\mathbf{E_c}$. This situation is represented on the total energy curves of Figure 5 by the coarse-dashed line lying along the x axis; thus the ony non zero contribution to total energy comes from $q\Phi_I$. Particles with $W = -1$ will flow along lines of $q\Phi_I$ = const. This can also be thought of as letting the radius of the circle in Figure 3c tend to infinity; hence all trajectories are bound to Io.

Apart from this one value of W there is always some background azimuthal drift. The rate of aborption of particles can easily be estimated by taking the product of the cross section ($2x_\infty$) with the y velocity component at $y = \pm\infty$ ($V_{y\infty}$) and the mass density ($\rho_0(W)$) per unit area in the equatorial plane at infinity.

$$\dot{m}(W) = 2x_\infty V_{y\infty}\rho_0(W) \tag{24}$$

where $\dot{m}(W)$ is the rate of mass absorption at W. The y velocity component at $y = \pm\infty$ (from (10)) is

$$\begin{aligned} V_{y\infty} &= (1/B_{eq}^2).\mathbf{B}_{eq}\wedge\nabla(-E_cR_Ix + w(x)/q) \\ &= -\hat{\mathbf{y}}.(E_c/B_{eq}).[W+1] \end{aligned} \tag{25}$$

since $\Phi \to -E_cR_Ix$ as $y \to \pm\infty$. Substituting this expression in (24) we can define the following quantity:

$$\dot{M} = \dot{m}/(2\rho_0).(B_{eq}/E_c) = x_\infty.[W+1] \tag{26}$$

TABLE 1. Summary of Drift Path Data

Range of $[W+1]/h$	x_∞	$\dot{M}$	Species	Type of Drift in Figure 3	Comments
>1	$1 - h/[W+1]$	$W + 1 - h$	protons electrons	a,b	Particles always repelled. $V_{y\infty}$ negative.
$0 \to 1$	0	0	protons electrons	c	Particles are excluded from within $r_o^2 = h/[W+1]$ of Io. $V_{y\infty}$ negative.
$-\frac{1}{2} \to 0$	$2\left\lvert\frac{-h}{W+1}\right\rvert^{\frac{1}{2}}$	$2\{-h[W+1]\}^{\frac{1}{2}}$	electrons	d	Particles are always attracted. Bound trajectories near $(\pm 1,0)$. Singularity in flow at $(\pm x_\infty/2,0)$. $V_{y\infty}$ positive.
$< -\frac{1}{2}$	$1 - h/[W+1]$	$W + 1 - h$	electrons	e,f	Particles always attracted. $V_{y\infty}$ positive.

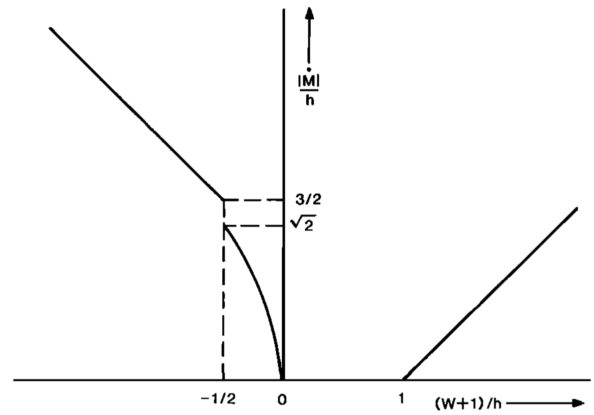

Fig. 7. The rate of mass absorption as a function of $[W+1]/h$: $\dot{M}$ has been normalized in such a manner that it represents the area (in the equatorial plane) swept per unit time.

$\dot{M}$ is normalized to the density of particles at W and the plasma convection velocity, so it really represents the area (in the equatorial plane) swept per unit of time. Table 1 shows the expressions for x_∞ and $\dot{M}$ for the various regimes of W. Figure 7 indicates the form of $\dot{M}$. This figure shows the same trends anticipated by Thomsen [1979] who plotted the particle lifetime against kinetic energy for different values of satellite conductivity. The model presented here provides a framework for a more quantitative description.

Comparison of Expected and Observed Particle Distribution

The absorption of particles by the process discussed in this paper will effect the distribution of particles around Io and its flux tube and Io's L shell. However, due to other physical processes such as L shell diffusion and torus absorption whose effects have not been estimated, it is difficult to comment on the bulk of particle data from the Pioneer an Voyager missions. One exception is the electron data reported by Lanzerotti et al. [1981]. These come from a pass of Voyager 1 with the Io flux tube region, and it is plausible to expect the interaction with the Alfvén wing to dominate when in such close proximity to Io's flux tube. Figure 8 shows electron distributions during an encounter with the flux tube region of Io. The dashed lines represent isotropic distributions. Between 1450 UT and 1503 UT Voyager 1 was approaching Io, and was receding during the interval 1504 UT to 1520 UT. The latitudes of Io and Voyager were 5.3° and 8.0° respectively. The decrease in electron number density can be understood by the energy dependence of the drifts. Goldstein and Ip [1983] predicted that 10 MeV electrons would execute the drift paths shown in Figure 3c. They explained how the "forbidden zone" would produce the decrease in electron number density near Io's flux tube reported by Lanzerotti et al. [1981]. However, no explanation of the pancake nature of the distribution was forwarded. Southwood et al. [1980] suggested that an internal satellite magnetic field could mirror particles outside the loss cone and give rise to such a distriubtion. Within the more general model we have presented here it is possible to explain both the pitch angles and number densities observed in the

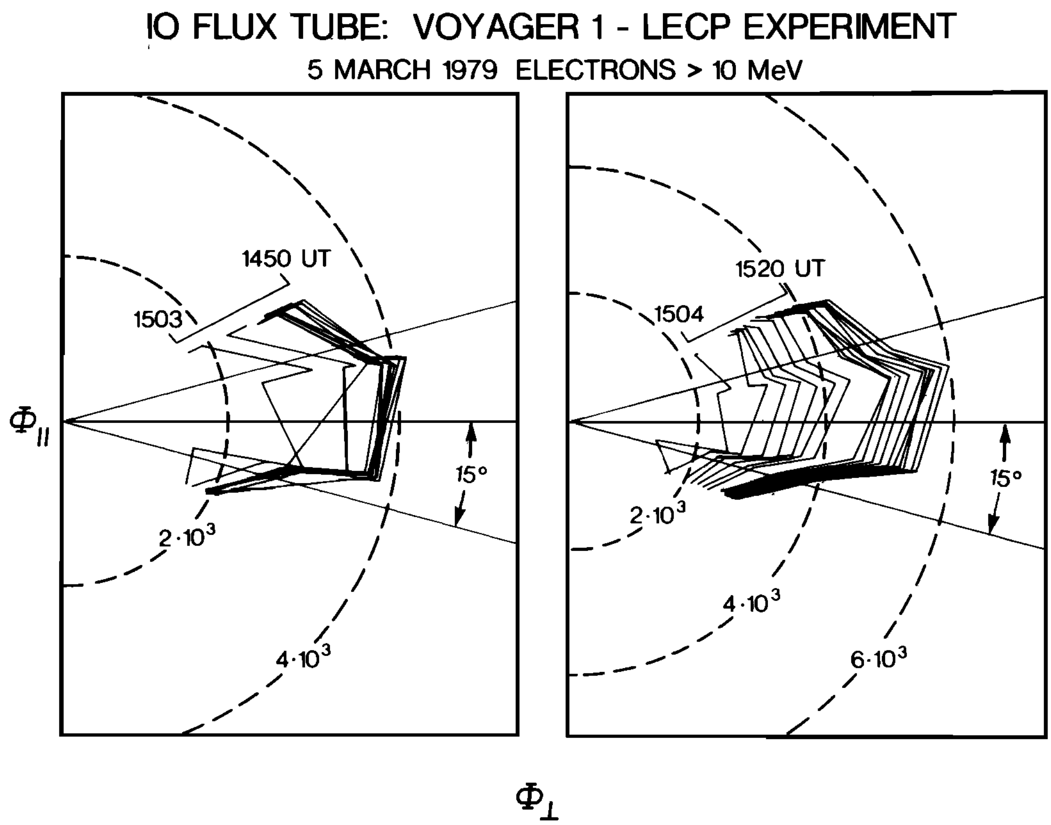

Fig. 8. The electron distribution during an encounter with the Io flux tube region [after Lanzerotti et al., 1981].

vicinity of Io. To do this we must first decide which flow from Figure 3 10 MeV electrons will execute. It is possible for Figures 3c, 3d, 3e or 3f to occur, depending upon the value of h. The flow mode of Figure 3c will result if h exceeds 0.4 (for $\alpha_0 = 0°$) or 0.14 (for $\alpha_0 = 90°$). It is difficult to estimate the value of h without knowledge of how Io's Alfvén waves propagate through the Io torus, but it is likely to be large enough to satisfy these criteria [Acuña et al., 1981; Hill et al., 1983]. A numerical study of Alfvén wave propagation is in progress. The radius of the exclusion circle in Figure 3c is determined by the particles charge, kinetic energy and equatorial pitch angle in addition to the satellite conductivity and Aflvén wave structure. On approaching Io the number of electrons that are excluded increases, and the magnitude of the electron distribution decreases. However, the peaking of the distribution throughout about 90° pitch angle is at first surprising since the exclusion at a given energy is more efficient for large pitch angle particles (cf. equation 14)).

Small pitch angle particles will mirror at high latitudes outside the torus, and it is important to remember that the electric field perturbation experienced by such particles will be strongly influenced by the propagation characteristics of the Alfvén wave through the torus. From the WKB approximation the amplitude of the Alfvén wave velocity perturbation would be expected to increase by a factor of about 4. In this instance particles that mirror outside the torus will be perturbed much more (h increases), and the exclusion radius will increase. As a result of this more particles with large pitch angles are anticipated. It is interesting to note that the "cut off" in pitch angle around 75° corresponds to particles mirroring at a latitude of 10° which is in close agreement with the present estimates of the torus boundary.

The range of the electron detectors on Voyager 1 did not go above 20 MeV. This is unfortunate for this study because electrons above this energy will execute the flow mode in Figure 3d, and at even higher energies those in Figures 3e and 3f. Since the outbound pass of Voyager 1 was upstream (with respect to the bulk plasma flow), these electrons would have shown a very significant drop in flux in the shadow region upstream of Io.

The main signatures from a wake pass will be in all the ion channels and possibly the low energy electron channels. These particles will have a shadow region downstream of Io, and a drop in particle flux is expected. The 10–MeV electrons have already been discussed. Hopefully missions such as Galileo will shed some light on these predictions and yield more information about the Io interaction. It should be remembered that we have not taken into account the existence of a tail behind Io in which newly created plasma is accelerated up to corotation speed. This will extend the source of Alfvén waves behind Io and require that we use a different expression for the electrostatic potential (equation (6)). However, the general trends anticipated are the same, unless the tail is also a source of electrons and ions in the energy range of interest. The pitch angle distribution should be consistent with the smaller pitch angles being perturbed the most. It should be remembered that our model has Io at the magnetic equator. This is not always the case and will result in particles with an equatorial pitch angle near 90 degrees being swept less efficiently in practice.

As more data are accumulated from the Io flux tube region, it may be possible to deduce some properties of the torus density distribution along the L shell of Io and also put some limits on Io's (or its ionosphere's) conductivity.

Conclusions

The theory of satellite sweeping has been studied with particular emphasis on the effect that Alfvén waves have on test particle trajectories. Unlike previous work [Schulz and Eviatar, 1977; Goldstein and Ip. 1983] our appraoch is analytical. This is made possible by our use of an empirical relation for the kinetic energy under conservation of the first and second adiabatic invariants [Hamlin et al., 1961' Southwood and Kivelson, 1975]. The analysis extends the existing models by including pitch angle dependence. This refinement makes it necessary to include latitudinal variation of the Alfvén wing and the different drift rates experienced by particles mirroring outside the magnetic equatorial plane. Certain features of the electron distribution observed near Io's flux tube can be understood using this model. For the first time an explanation of the pancake nature of the distribution has been advanced, without invoking satellite magnetization [Southwood et al., 1980], and appears to be in accord with the observations.

This decription of particle motion past Io should provide a useful framework for interpreting particle data from passes of the Io flux tube region. Various signatures in the electron and proton distributions have been advanced, and most of these will have to wait for Galileo until further discussion is possible.

Acknowledgments. The author is grateful to D. J. Southwood who proposed and conceived the original line of research. M. G. Kivelson and D. J. S. are thanked for useful discussions and comments. This research was supported by a UK Science and Engineering Research Council studentship.

The Editor thanks L. L. Hood, M. F. Thomsen, and a third referee for their assistance in evaluating this paper.

References

Acuña, M. H., F. M. Neubauer, and N. F. Ness, Standing Alfvén wave current system at Io: Voyager 1 observations, J. Geophys. Res., 86, 8513, 1981.

Alfvén, H., and C. -G. Falthammar, Cosmical Electrodynamics, Oxford University Press, New York, 1963.

Belcher, J. W., The low energy plasma in the Jovian Magnetosphere, in Physics of the Jovian Magnetosphere, edited by A. J. Dessler, Cambridge University Press, New York, 1983.

Bell, E. V., II, and T. P. Armstrong, Monte Carlo simulation of charged particle impact on the satellites of Jupiter and Saturn, J. Geophys. Res, 91, 1397, 1986.

Drell, S. D., H. M. Foley, and M. A. Ruderman, Drag and propulsion of large satellites in the ionosphere, J. Geophys. Res, 70, 3131, 1965.

Geortz, C. K., Io's interaction with the plasma torus, J. Geophys. Res., 85, 2949, 1980.

Goldreich, P., and D. Lydnen-Bell, Io, a Jovian unipolar inductor, Astrophys. J., 156, 59, 1969.

Goldstein, B. E., and W. -H. Ip, Magnetic drifts at Io: Depletion of 10-MeV electrons at Voyager 1 encounter due to a forbidden zone, J. Geophys. Res., 88, 6137, 1983.

Hamlin, D. A., R. Karplus, R. C. Vik, and K. M. Watson, Mirror and azimuthal drift frequencies for geomagnetically trapped particles, J. Geophys. Res., 66, 1, 1961.

Hill, T. W., A. J. Dessler, and C. K. Goertz, Magnetospheric models, in Physics of the Jovian Magnetosphere, edited by A. J. Dessler, Cambridge University Press, New York, 1983.

Hood, L. L., Radial diffusion of low energy ions in Saturn's radiation belts: A combined analysis of phase space density and satellite microsignature data, J. Geophys. Res., 90, 6295, 1985.

Lanzerotti, L. J., C. G. Maclennan, T. P. Armstrong, S. M. Krimigis, R. P. Lepping, and N. F. Ness, Ion and electron angular distributions in the Io torus region of the Jovian magnetosphere, J. Geophys. Res., 86, 8491, 1981.

Mogro-Campero, A., and R. W. Fillius, The absorption of trapped particles by the inner satellites of Jupiter and the radial diffusion coefficient of particle transport, J. Geophys. Res., 81, 1289, 1976.

Neubauer, F. M., Nonlinear standing Alfvén wave current system at Io: Theory, J. Geophys. Res., 85, 1171, 1980.

Paonessa, M., and A. F. Cheng, A theory of satellite sweeping, J. Geophys. Res., 90, 3428, 1985.

Paonessa, M., and A. F. Cheng, Limits on ion radial diffusion coefficients in Saturn's inner magnetosphere, J. Geophys. Res., 91, 1391, 1986.

Schardt, A. W., and C. K. Goertz, High energy particles, in Physics of the Jovian Magnetosphere, edited by A. J. Dessler, Cambridge University Press, New York, 1983.

Schulz M., and A. Eviatar, Charged particle absorption by Io, Astrophys. J. Lett., 211, L149, 1977.

Southwood, D. J., and M. W. Dunlop, Mass pickup in sub-Alfvénic plasma flow: A case study for Io, Planet. Space Sci., 32, 1079, 1984.

Southwood, D. J., and M. G. Kivelson, An approximate analytic description of plasma bulk parameters and pitch angle anisotropy under adiabatic flow in a dipolar magnetospheric field, J. Geophys. Res., 80, 2069, 1975.

Southwood, D. J., M. G. Kivelson, R. J. Walker, and J. A. Slavin, Io and its plasma environment, J. Geophys. Res., 85, 5959, 1980.

Thomsen, M. F., Jovian magnetosphere- satellite interactions: Aspects of energetic charged particle loss, Rev. Geophys., 17, 369, 1979.

Thomsen, M. F., C. K. Goertz, and J. A. Van Allen, On determining magnetospheric diffusion coefficients from the observed effects of Jupiter's satellite Io, J. Geophys. Res., 82, 5541, 1977.

Wright, A. N., and D. J. Southwood, Stationary Alfvénic Structures, J. Geophys. Res., in press, 1987.

A. N. Wright, Theoretical Astronomy Unit, School of Mathematical Sciences, Queen Mary College, London E1 4NS, England.

(Received May 30, 1986;
revised October 3, 1986;
accepted October 30, 1986.)